Available online at www.sciencedirect.com
SCIENCE DIRECT
Polymer 46 (2005) 1609–1616
polymer
www.elsevier.com/locate/polymer

Steady-state fluorescence and NMR study on self-association behavior of poly(methacrylamides) bearing hydrophobic amino acid residues

Akihito Hashidzume, Akira Harada*

Department of Macromolecular Science, Graduate School of Science, Osaka University, 1-1 Machikaneyama-cho, Toyonaka, Osaka 560-0043, Japan

Received 5 July 2004; received in revised form 1 December 2004; accepted 8 December 2004
Available online 22 December 2004

Abstract

Self-association properties of poly(*N*-methacryloylphenylalanine) and poly(*N*-methacryloyltryptophan) (pMPhe and pMTrp, respectively) were investigated by several characterization techniques, including steady-state fluorescence and NMR. These characterization data revealed similarities and distinctions of their self-association properties.

The pH dependencies of association properties of pMPhe and pMTrp are practically the same. Apparent pK_a values for pMPhe and pMTrp were determined to be 5.7 and 5.8, respectively, by potentiometric titration. Steady-state fluorescence measurements at varying pH using pyrene as fluorescence probe indicated that, at pH ≈ 5 (< apparent pH), hydrophobic microdomains were formed, while, at pH ≈ 7 and 9 (> apparent pK_a), hydrophobic microdomains were not formed significantly. ^{1}H NMR spectra for both the polymers measured in D_2O exhibited that a significant fraction of aromatic rings in amino acid residues were located close to the polymer main chain, and that, at pH ≈ 5, the mobility of the polymer main chain and the aromatic ring was extremely restricted.

The polymer concentration (C_p) dependencies of association properties of pMPhe and pMTrp at pH ≈ 5 are distinct. Steady-state fluorescence data at varying C_p indicated that pMPhe was more hydrophobic microscopically than pMTrp. Dynamic light scattering data indicated that pMTrp had a stronger tendency for interpolymer association than pMPhe did at pH ≈ 5. It is concluded that the distinction in C_p dependency of the self-association properties of pMPhe and pMTrp is due to the differences in the bulkiness and the hydrophobicity of the substituents of amino acid residues.

Keywords: Self-association behavior; Poly(*N*-methacryloyl-amino acids); Hydrophobic amino acid residues

1. Introduction

Various functions of proteins are expressed by the formation of their higher-order structures controlled precisely and delicately by noncovalent bonds between amino acid residues, including hydrogen bonding, electrostatic interaction, and hydrophobic interaction [1]. In order to utilize these noncovalent bonds between amino acid residues for the self-association behavior of synthetic polymers, we have been focusing on poly{(meth)acrylamides} bearing amino acid residues. Polymers of *N*-(meth)acryloyl-amino acids have been synthesized and studied by many research groups because of their relevance to proteins [2]. To our knowledge, however, there have been only a few papers concerning the self-association behavior of poly{*N*-(meth)acryloyl-amino acids} in aqueous media with a focus on hydrophobic interaction [3–5].

In order to investigate the self-association behavior of poly(*N*-methacryloyl-amino acids) with a focus on hydrophobic interaction, we have chosen phenylalanine (Phe) and tryptophan (Trp) as amino acid residues in the present study. This is because Phe and Trp are most hydrophobic amino acids according to the hydrophilicity values reported by Hopp and Woods [6]. Furthermore, since Phe and Trp have aromatic rings, respectively, associations may occur not only through hydrophobic interaction but also through π–π or CH–π interaction.

Our preliminary results of solubility test for homopolymers of *N*-methacryloylphenylalanine and *N*-methacryloyltryptophan (pMPhe and pMTrp, respectively, in Scheme 1)

* Corresponding author. Tel./fax: +81 6 6850 5445.
E-mail address: harada@chem.sci.osaka-u.ac.jp (A. Harada).

0032-3861/$ - see front matter © 2004 Elsevier Ltd. All rights reserved.
doi:10.1016/j.polymer.2004.12.011

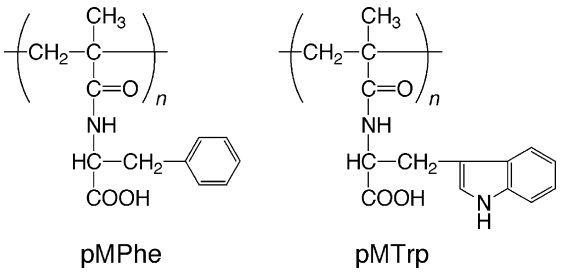

Scheme 1. Structures of the polymers used in this study.

indicated that pMPhe (sodium salt) was more soluble in acidic media than pMTrp (sodium salt), indicating that a subtle difference of the substituents in amino acid residues causes some distinction of their self-association properties. Elucidation of structural factors for the distinction in association properties may give us some insights for precise and delicate control of the association behavior of synthetic polymers. Therefore, in this paper, we investigate the self-association behavior of pMPhe and pMTrp by several characterization techniques, including steady-state fluorescence and NMR, and describe similarities and distinctions of their self-association properties. On the basis of these characterization data, we discuss structural factors which cause the distinction in association properties of pMPhe and pMTrp.

2. Experimental

2.1. Materials

L-Phenylalanine (SAJ), L-tryptophan (SAJ), and methacryloyl chloride (Wako) were used without further purification. Methanol (Wako) used as solvent for polymerization was purified by distillation over magnesium under an argon atmosphere. 2,2′-Azobis(isobutyronitrile) (AIBN) (Wako) was recrystallized from methanol. Milli-Q water was used to prepare aqueous polymer solutions. Pyrene (Wako) was recrystallized twice from ethanol. Other reagents were used without further purification.

The monomers used in this study, *N*-methacryloylphenylalanine (MPhe) [3] and *N*-methacryloyltryptophan (MTrp) [7], were prepared from methacryloyl chloride and the corresponding amino acids, respectively, according to the literatures.

2.2. Polymerization

Typical procedure for radical polymerization is described below.

MPhe (3.0 g, 13 mmol) and AIBN (20 mg, 0.12 mmol) were dissolved in methanol (15 ml) under an argon atmosphere. The solution was warmed with an oil-bath thermostated at 70 °C. After 24 h, ethyl acetate (ca. 150 ml) was poured into the mixture to obtain polymer of MPhe (pMPhe) as precipitate. The polymer obtained was purified by reprecipitation from a methanol solution into excess ethyl acetate, and was dried in vacuo: yield 2.2 g, 75%. IR (KBr) ν_{max}: 3424 (amide NH), 3089 (aromatic CH), 3064 (aromatic CH), 3031 (aromatic CH), 2933 (aliphatic CH), 1734 (amide C=O), 1642 (aromatic ring), 1519 (aromatic ring). ^{1}H NMR (400 MHz, CD_3OD): δ −0.3–2.4 (α-CH_3 and CH_2 in the polymer main chain), 2.6–4.0 (CH_2 in the phenylalanine residue), 4.5–4.8 (CH in the phenylalanine residue) 6.3–8.4 (amide NH), 6.9–7.5 (aromatic protons). Calcd for $(C_{13}H_{15}NO_3)(H_2O)_{0.6}$: C, 63.97; H, 6.69; N, 5.74. Found: C, 63.92; H, 6.61; N, 5.67.

The polymer of MTrp (pMTrp): yield 2.3 g, 76%. IR (KBr) ν_{max}: 3414 (amide NH), 3082 (aromatic CH), 3058 (aromatic CH), 2927 (aliphatic CH), 1729 (amide C=O), 1629 (aromatic ring), 1514 (aromatic ring). ^{1}H NMR (400 MHz, CD_3OD): δ −0.8–2.5 (α-CH_3 and CH_2 in the polymer main chain), 2.5–4.1 (CH_2 in the tryptophan residue), 4.2–5.0 (CH in the tryptophan residue), 6.0–8.5 (amide NH), 6.8–7.8 (aromatic protons). Calcd for $(C_{15}H_{16}N_2O_3)(H_2O)_{0.65}$: C, 63.44; H, 6.14; N, 9.86. Found: C, 63.42; H, 6.42; N, 9.68.

For characterization in aqueous media, both the polymers were neutralized with an equimolar amount of 0.10 M NaOH, and then recovered by freeze-drying.

2.3. Measurements

2.3.1. IR

IR spectra were recorded on a JASCO FT/IR-410 spectrometer using KBr disks.

2.3.2. Gel permeation chromatography (GPC)

GPC measurements were carried out at 40 °C on a TOSOH CCP and 8010 system equipped with two TOSOH TSKgel MultiporeH_{XL}-M columns connected in series, using THF as eluent at a flow rate of 0.8 ml/min. TOSOH UV-8010 and TOSOH RI-8012 detectors were used. Molecular weights were calibrated with polystyrene standards (TSK standard POLYSTYRENE). For GPC measurements, polymers esterified with diazomethane according to the conventional procedure [8] were used.

2.3.3. Turbidimetric and potentiometric titrations

The polymer samples not neutralized (0.20 mmol monomer units) were dissolved in 0.10 M NaOH (2.0 ml) and then diluted with water (18 ml). While these polymer solutions were titrated with 0.10 M HCl using a microburet at 25 °C, turbidity and pH were monitored. Turbidities, reported as $100-\%T$, were measured with a Brinkmann PC920 probe colorimeter equipped with a 1 cm path length fiber optics probe at 450 nm. Values of pH were measured with a Horiba F-23 pH meter equipped with a Horiba 6366-10D glass electrode. The reference electrode was calibrated with buffer solutions of pH 4, 7, and 9 prior to pH measurements. The degrees of neutralization (α) were

calculated from the amounts of the monomer unit and the added HCl.

2.3.4. Steady-state fluorescence

Steady-state fluorescence spectra were measured on a Hitachi F-4500 fluorescence spectrophotometer using a 1 cm path length quartz cuvette. Excitation spectra for pyrene solubilized in aqueous polymer solutions were monitored at 372 nm. Emission spectra were measured with excitation at 333 nm. The slit widths for both excitation and emission sides were kept at 2.5 nm during measurement.

For fluorescence measurements at varying pH, the neutralized polymers were dissolved in pyrene-saturated 0.05 M NaCl and then heated at >90 °C for ca. 10 min. After these polymer solutions were cooled down to room temperature, pH values were adjusted by adding a small amount of pyrene-free 0.10 M HCl or 0.10 M NaOH using a microburet. For fluorescence measurements at varying polymer concentrations (C_p), stock solutions containing 10 g/l polymer were prepared by dissolving the neutralized polymers in a pyrene-saturated buffer solution (pH $\approx$ 5, 7, or 9, the ionic strength = 0.05) at >90 °C for ca. 10 min. After cooling down to room temperature, these stock solutions were diluted with a pyrene-saturated buffer solution of the same pH to adjust C_p, and then were heated at >90 °C for ca. 10 min.

Pyrene-saturated aqueous solutions were prepared as follows: A few drops of a solution of pyrene in acetone (ca. 0.03 M) were poured into an aqueous NaCl or buffer solution (100 ml). After this mixture was sonicated for ca. 6 h at ca. 60 °C, precipitate was removed by filtration with a 0.45 μm pore size membrane filter. We confirmed the absence of pyrene excimer fluorescence for all the pyrene-saturated aqueous solutions before preparation of polymer solutions.

2.3.5. ^{1}H NMR

One-dimensional ^{1}H NMR spectra for the polymers were measured on a JEOL JNM GSX400 or EX270 spectrometer in methanol-d_4 or D_2O at 30 °C. Two-dimensional nuclear Overhauser effect spectroscopy (NOESY) measurements were carried out with a Varian Unity INOVA 600 spectrometer in D_2O. Mixing time before the acquisition of free induction decay was carefully varied and fixed to 10 ms to obtain a genuine NOE and to avoid the effect of spin diffusion.

For measurements in D_2O, the neutralized polymer samples were dissolved in D_2O containing 0.05 M NaCl. Values of pH were adjusted to ca. 5, 7, and 9, respectively, by adding a small amount of 0.10 M HCl or 0.10 M NaOH, and then sample solutions were heated at >90 °C for ca. 10 min. Chemical shifts were determined using acetonitrile as an external standard (2.0 ppm).

2.3.6. Dynamic light scattering (DLS)

DLS measurements were carried out at 25 °C using an Otsuka Electronics Photal DLS-7000 light scattering spectrometer equipped with an argon ion laser (50 mW at 488 nm) and detector optics. An ALV-5000E digital multiple τ correlator (Langen-GmbH) was used for data collection. To obtain distributions of apparent hydrodynamic radius (R_h), the inverse Laplace transform analysis was performed utilizing the REPES algorithm [9], followed by conversion of relaxation time into R_h using the Einstein–Stokes relation. Sample solutions were prepared by dissolving the neutralized polymers in a buffer solution (pH $\approx$ 5, the ionic strength = 0.05) at >90 °C for ca. 10 min. After cooling down to room temperature, these sample solutions were filtered with a 0.8 μm pore size membrane filter.

3. Results and discussion

3.1. Basic characteristics of pMPhe and pMTrp

The monomers used in this study, MPhe [3] and MTrp [7], were prepared from methacryloyl chloride and the corresponding amino acids, respectively, according to the literatures. These monomers were polymerized using AIBN in methanol under an argon atmosphere at 70 °C for 24 h. The polymers obtained, pMPhe and pMTrp, were purified by reprecipitation from a methanol solution into excess ethyl acetate. Both pMPhe and pMTrp were soluble in basic water, methanol, ethanol, *N*,*N*-dimethylformamide, dimethyl sulfoxide, THF, and 1,4-dioxane, and were insoluble in neutral water, acetone, diethyl ether, ethyl acetate, chloroform, dichloromethane, benzene, toluene, and hexane. As listed in Table 1, M_n values for pMPhe and pMTrp esterified with diazomethane were determined to be 3.1×10^4 and 5.1×10^4, respectively, by GPC. Since the molecular weight distributions for pMPhe and pMTrp were rather broad ($M_w/M_n = 1.5$ and 1.4 for pMPhe and pMTrp, respectively), the molecular weight ranges for both the polymers considerably overlap. Thus, it is likely that the difference in M_n values causes no distinctions in the self-association properties of these polymers. Since pMPhe and pMTrp not neutralized were unable to be dissolved in neutral water directly, these polymers were neutralized with an equimolar amount of 0.10 M NaOH for measurements in aqueous media.

Table 1
M_n and M_w/M_n for pMPhe and pMTrp used in this study

Polymer code	$M_n\times10^{-4}$ [a]	M_w/M_n [a]
pMPhe	3.1	1.5
pMTrp	5.1	1.4

[a] Determined for polymers esterified with diazomethane by GPC in THF. Molecular weights were calibrated using polystyrene standards.

To examine the pH ranges in which the polymers were soluble in water and to determine their apparent pK_a values, turbidimetric and potentiometric titrations were carried out. Fig. 1 shows turbidimetric and potentiometric titration data for pMPhe and pMTrp with adding 0.10 M HCl to aqueous solutions of the polymers neutralized with an equimolar amount of NaOH. As pH is decreased, turbidity starts to increase slightly at pH≈6, and then starts to increase markedly at pH≈4.2. From the potentiometric titration data, apparent pK_a values for pMPhe and pMTrp were determined to be 5.7 and 5.8, respectively. Comparison of these turbidimetric and potentiometric titration data indicates that pH values at the onset of the slight increase in turbidity correspond well to the apparent pK_a values, and that both the polymers are insoluble in water at $\alpha <$ ca. 0.1.

3.2. Steady-state fluorescence

Since pMPhe did not emit significant fluorescence, pyrene was used as fluorescence probe to investigate the formation of hydrophobic microdomains. It is well-known that steady-state fluorescence excitation and emission spectra for pyrene are dependent on the polarity of the microenvironment around pyrene probes [10,11]. Fig. 2 shows steady-state fluorescence excitation spectra for pyrene solubilized in 1.0 g/l pMPhe at varying pH. In the pH range 6.0–10.2, these spectra show three bands due to pyrene at ca. 304, 318, and 333 nm, respectively, independent of pH. On the other hand, at pH 4.8, the three bands are seen at longer wavelengths (i.e. ca. 309, 322, and 338 nm, respectively), indicating that pyrene probes are solubilized

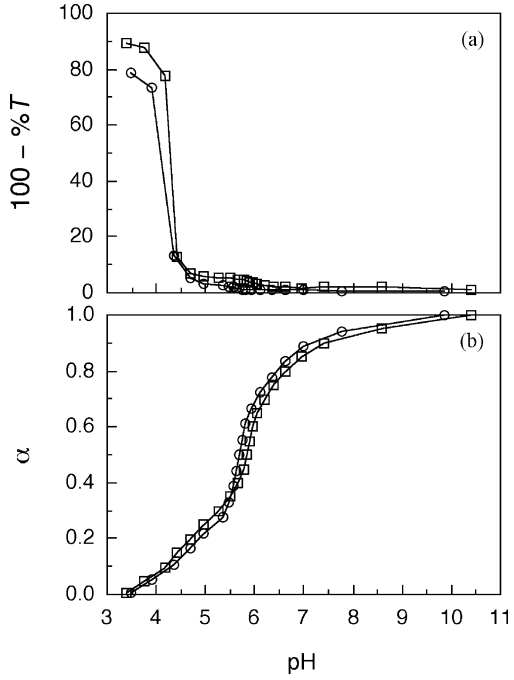

Fig. 1. Turbidimetric (a) and potentiometric (b) titration data for pMPhe (○) and pMTrp (□). Initial amount of aqueous solution = 20 ml, titrant: 0.10 M HCl.

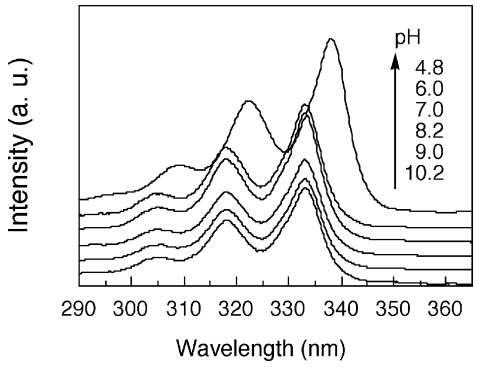

Fig. 2. Steady-state fluorescence excitation spectra for pyrene solubilized in 1.0 g/l pMPhe at varying pH.

markedly in hydrophobic media [10]. This observation is indicative of the formation of hydrophobic microdomains at pH 4.8. From these spectra, the ratios (I_{338}/I_{333}) of the fluorescence intensity at 338 nm and that at 333 nm were calculated and plotted against pH, as shown in Fig. 3. In the pH region 6–10 (> apparent pK_a), I_{338}/I_{333} is constant (≈0.3) independent of pH, while I_{338}/I_{333} increases markedly up to ca. 1.8 with decreasing pH down to ca. 5. These plots indicate that hydrophobic microdomains are formed at pH < apparent pK_a.

We also measured steady-state fluorescence at varying C_p in acidic, neutral, and basic media (pH≈5, 7, and 9, respectively). As an example, Fig. 4 shows steady-state fluorescence excitation and emission spectra for pyrene solubilized in pMPhe of varying C_p at pH≈5. In steady-state excitation spectra (Fig. 4(a)), the intensities of bands at ca. 309, 322, and 338 nm due to pyrene probes incorporated in hydrophobic microdomains increase with increasing C_p. This observation indicates that the fraction of pyrene probes incorporated in hydrophobic microdomains increases remarkably with increasing C_p at pH≈5 [10]. Values of I_{338}/I_{333} were calculated using the excitation spectra and plotted against C_p at pH≈5, 7, and 9, as shown in Fig. 5(a). At pH≈7 and 9, I_{338}/I_{333} is constant (≈0.3) at $C_p < 10^0$ g/l, but, at $C_p \geq 10^0$ g/l, I_{338}/I_{333} increases only slightly, indicating that pyrene probes are incorporated into

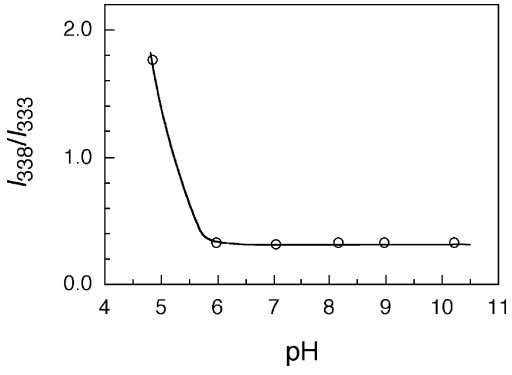

Fig. 3. I_{338}/I_{333} as a function of pH for pyrene solubilized in 1.0 g/l pMPhe at [NaCl] = 0.05 M.

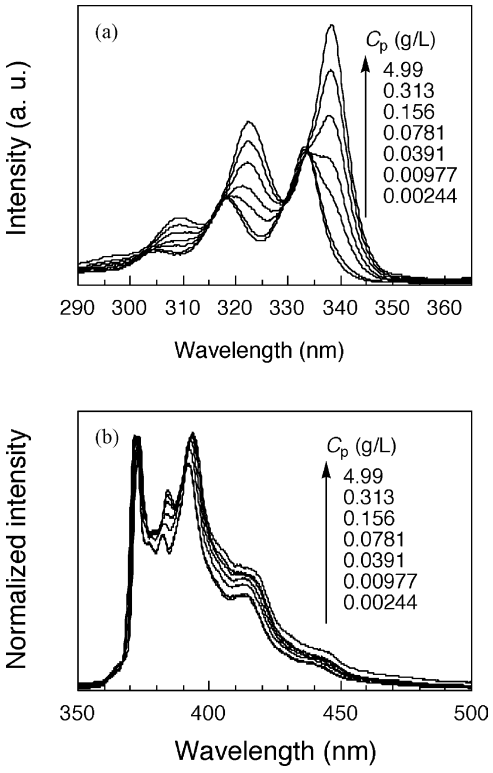

Fig. 4. Steady-state fluorescence excitation (a) and emission (b) spectra for pyrene solubilized in pMPhe of varying C_p at pH≈5 and $I=0.05$.

relatively hydrophobic environments formed by pMPhe at $C_p \geq 10^0$ g/l. Since, in a separate experiment, I_{338}/I_{333} for pyrene solubilized in aqueous solutions of poly(sodium methacrylate) increased only slightly at $C_p \geq 10^0$ g/l, the slight increase in I_{338}/I_{333} at pH≈7 and 9 may be induced by association of α-methyl groups. On the other hand, at pH≈5, I_{338}/I_{333} starts to increase at $C_p \approx 5\times10^{-3}$ g/l. As C_p is further increased, I_{338}/I_{333} increases remarkably in the C_p range 10^{-2}–10^0 g/l, and then levels off at ca. 2.0 when $C_p \geq 10^0$ g/l. These data indicate that, at pH≈5, pMPhe forms hydrophobic microdomains, while, at pH≈7 and 9, it does not form hydrophobic microdomains considerably.

In order to clarify whether a single pMPhe chain forms a hydrophobic microdomain or not, at an extremely low C_p, we calculated the ratio of the pyrene concentrations in the hydrophobic phase and in the bulk water phase ($[Py]_m/[Py]_w$) using the data shown in Fig. 5a by assuming the minimum and maximum values of I_{338}/I_{333} at low and high C_p, respectively, and were plotted in Fig. 6 against C_p for pMPhe at pH≈5 [10]. The plots show a break in a low C_p region (inset in Fig. 6) which corresponds to the onset of interpolymer associations, indicating that pyrene probes are incorporated much more efficiently in interpolymer aggregates than in intrapolymer ones, and that a hydrophobic microdomain is formed by a plural number of polymer chains presumably through intra- and interpolymer associations. From the break shown in the inset of Fig. 6, the onset C_p for interpolymer association (i.e. apparent cmc) was estimated to be 1.4×10^{-3} g/l (5.6×10^{-6} M MPhe units) for pMPhe at pH≈5.

Fig. 4(b) exhibits normalized steady-state fluorescence emission spectra for pyrene solubilized in pMPhe of varying C_p at pH≈5. As shown in this figure, as C_p is increased, the intensity of the third vibronic peak gradually increases relative to that of the first vibronic peak, indicative of the formation of hydrophobic microdomains [11]. Using these emission spectra, the ratios (I_3/I_1) of the fluorescence intensity of the third vibronic peak and that of the first vibronic peak were also calculated and plotted against C_p at pH≈5, 7, and 9, as shown in Fig. 5(b). Similar to Fig. 5(a), Fig. 5(b) indicates that, at pH≈5, pMPhe forms hydrophobic microdomains considerably, while, at pH≈7 and 9, it does not. It should be noted here that the saturated value of I_3/I_1 (ca. 0.8) at pH≈5 is significantly smaller than that for

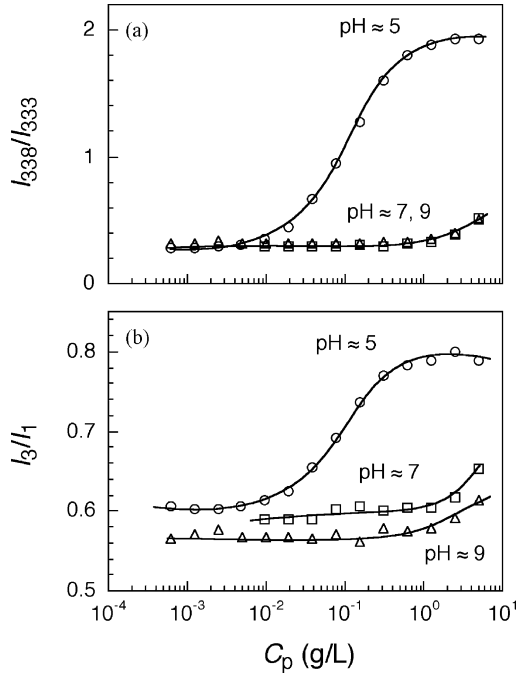

Fig. 5. I_{338}/I_{333} (a) and I_3/I_1 (b) as a function of C_p for pyrene solubilized in pMPhe at pH≈5, 7, and 9.

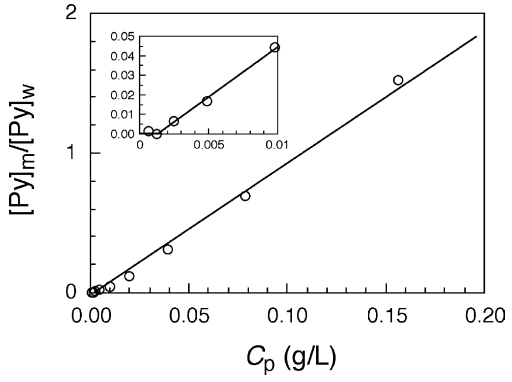

Fig. 6. $[Py]_m/[Py]_w$ calculated from I_{338}/I_{333} as a function of C_p for pMPhe at pH≈5. The inset shows plots for a low C_p region.

pyrene solubilized in conventional micelles of sodium dodecyl sulfate ($I_3/I_1 = 1.0$) [12]. This observation indicates that the microdomains in pMPhe are relatively less hydrophobic, suggesting that a significant fraction of carboxylic acid groups are incorporated in the microdomains.

In the case of pMTrp, we had expected that tryptophan residues in pMTrp could be used as fluorescence label, but C_p dependency of fluorescence spectra for pMTrp was independent of pH. This observation implies that the fluorescence monitored was due to tryptophan residues not associated because of strong self-quenching of associated ones. Thus, pyrene was also used as fluorescence probe to examine the formation of hydrophobic microdomains in pMTrp, although fluorescence spectra due to pyrene and tryptophan considerably overlapped. Excitation spectra were measured at $C_p \leq 0.626$ g/l, where the contribution of fluorescence from tryptophan residues was not large very much, and were corrected by subtracting of excitation spectra for pyrene-free pMTrp. Using the corrected spectra, I_{338}/I_{333} values were calculated and plotted against C_p in Fig. 7. At pH ≈ 7 and 9, I_{338}/I_{333} is constant (≈0.3) independent of C_p in the whole C_p region examined (0.0098–0.626 g/l). On the other hand, at pH ≈ 5, I_{338}/I_{333} starts to increase at $C_p \approx 1 \times 10^{-2}$ g/l as C_p is increased. Since these plots do not exhibit a saturation tendency at higher C_p, the onset C_p for interpolymer association for pMTrp was unable to be estimated. However, it is noteworthy that the C_p at which I_{338}/I_{333} starts to increase for pMTrp ($\approx 1 \times 10^{-2}$ g/l, ca. 4×10^{-5} M MTrp units) is higher than that for pMPhe ($\approx 5 \times 10^{-3}$ g/l, ca. 2×10^{-5} M MPhe units). These data indicate that the onset C_p for interpolymer association for pMTrp is higher than that for pMPhe, or that the partition coefficient of pyrene between hydrophobic microdomain pseudo-phase and bulk water phase for pMTrp is smaller than that for pMPhe [13]. Thus, these fluorescence data indicate that, at pH ≈ 5, pMPhe is more hydrophobic microscopically than pMTrp.

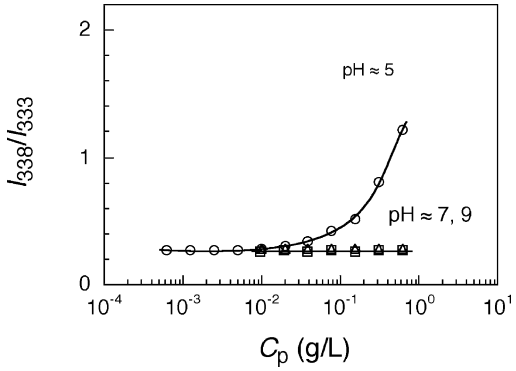

Fig. 7. I_{338}/I_{333} as a function of C_p for pyrene solubilized in pMTrp at pH ≈ 5, 7, and 9.

3.3. ^{1}H NMR

To investigate the microscopic structure and the mobility of pMPhe and pMTrp in aqueous media, ^{1}H NMR measurements were carried out using D_2O as solvent. Fig. 8 compares ^{1}H NMR spectra for 1.0 g/l pMPhe and pMTrp at pH ≈ 5, 7, and 9.

In the NMR spectra for pMPhe and pMTrp at pH ≈ 7, broad resonance bands in the region −1 to 2 ppm are due to α-methyl protons and methylene protons in the polymer main chain. Resonance bands ascribable to methylene and methine protons in the amino acid residue are seen around 3.5 and 4.5 ppm, respectively. The resonance bands in the region 6–8 ppm are assignable to aromatic protons in the amino acid residue. It is important to note that the resonance bands due to α-methyl protons and methylene protons in the polymer main chain range to the relatively high magnetic field region (<0 ppm), indicating that these protons are shielded by the ring current of the aromatic rings in the amino acid residues. This observation indicates that a significant fraction of aromatic rings in the amino acid residues are located close to the polymer main chain presumably because of hydrophobic and CH–π interactions [14]. To confirm the location of the aromatic rings close to the polymer main chain, NOESY experiments were performed for the same sample solutions of pH ≈ 7. NOESY spectra (Fig. 9) show genuine NOE signals between resonance bands due to the aromatic ring and

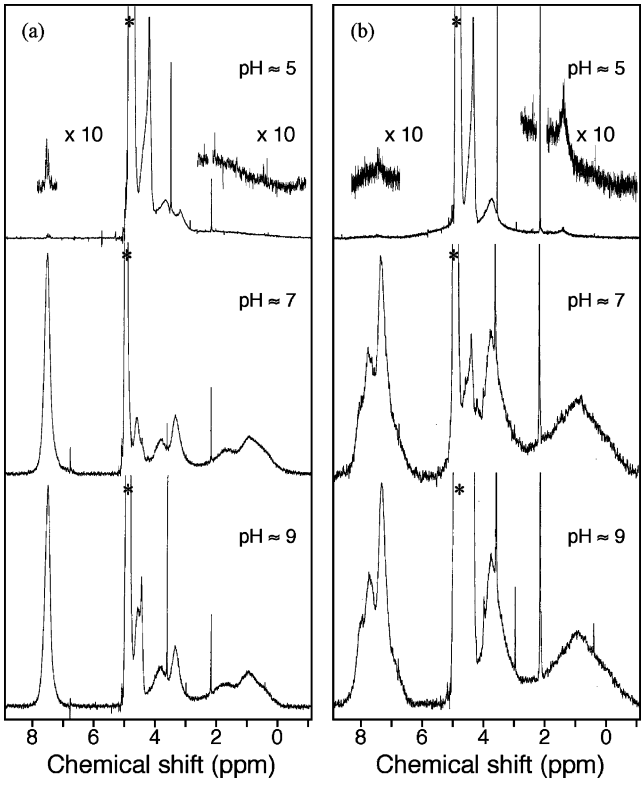

Fig. 8. ^{1}H NMR spectra for pMPhe (a) and pMTrp (b) in D_2O at pH ≈ 5, 7, and 9. Asterisks denote the resonance bands due to the solvent.

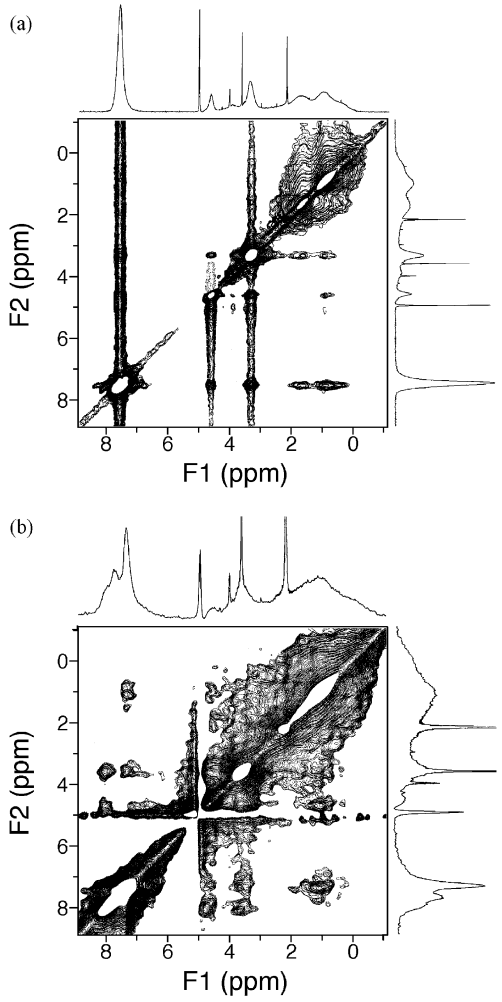

Fig. 9. NOESY spectra for pMPhe (a) and pMTrp (b) in D_2O at pH≈7.

those due to α-methyl protons and methylene protons in the polymer main chain for both the polymers. These NOESY data indicate that a significant fraction of the aromatic rings are located close to the polymer main chain.

As shown in Fig. 8, NMR spectra at pH≈9 are practically the same as those at pH≈7. In the spectra observed at pH≈5, however, resonance bands due to α-methyl protons, methylene protons in the polymer main chain, and aromatic protons are remarkably weak relative to the resonance bands due to methylene and methine protons in the amino acid residue. These spectra indicate that, at pH≈5, the mobility of the polymer main chain and the aromatic ring is highly restricted, resulting in an extremely fast spin–spin relaxation.

In the microscopic structures of pMPhe and pMTrp, hydrogen bonds of the amide protons may play an important role. The ^1H NMR spectra measured in D_2O did not allow us to examine the formation of hydrogen bonds of the amide protons, because no resonance bands due to the amide protons were observed in these spectra. However, in NMR spectra measured in methanol-d_4, broad resonance bands ascribable to the amide protons were observed in the regions 6.3–8.4 and 6.0–8.5 ppm for pMPhe and pMTrp, respectively (see Section 2), indicating that a significant amount of the amide protons were used for hydrogen bonding formation. Furthermore, in the spectra measured in methanol-d_4, the resonance bands due to α-methyl protons and methylene protons in the polymer main chain also ranged to the relatively high magnetic field region (<0 ppm, see Section 2), indicating that a significant fraction of aromatic rings in the amino acid residues were located close to the polymer main chain. Since solvophobic interaction is much weaker in methanol than in water, the formation of hydrogen bonds of the amide protons may induce the location of aromatic rings close to the polymer main chain in methanol. On the basis of the NMR spectra measured in methanol-d_4, it can be considered that the formation of hydrogen bonds of the amide protons is also important for the self-association of pMPhe and pMTrp in aqueous media.

3.4. DLS

In order to investigate the extent of interpolymer association for pMPhe and pMTrp in acidic media, DLS measurements were carried out. Fig. 10 compares R_h distributions for pMPhe and pMTrp at pH≈5. For both the polymers, as C_p is increased, the fraction of larger aggregates increases. Especially, for pMTrp at $C_p \geq 2.5$ g/l, R_h distributions show two peaks at ca. 10^1 and 10^2 nm. These data indicate that, at pH≈5, pMTrp exhibits a stronger tendency for interpolymer association than pMPhe does.

3.5. Self-association behavior of pMPhe and pMTrp

On the basis of the data described above, we summarize

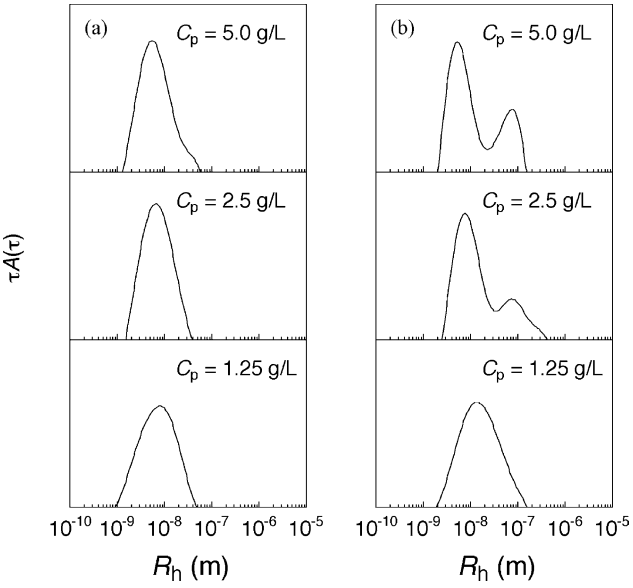

Fig. 10. R_h distributions for pMPhe (a) and pMTrp (b) of varying C_p at pH≈5. Scattering angle=90°.

here the self-association behavior of pMPhe and pMTrp in aqueous media.

The pH dependencies of association properties for pMPhe and pMTrp are practically the same. At pH > apparent pK_a, more than half of carboxyl groups are in the carboxylate anion state, and thus, the polymer chain carries a number of charges to adopt an extended conformation, in which hydrophobic microdomains are not formed significantly because of electrostatic repulsion. As indicated by the NMR data (Figs. 8 and 9), a significant fraction of aromatic rings are located close to the polymer main chain. When, at pH ≈ 5 (< apparent pK_a), carboxyl groups in the polymer chain become relatively hydrophobic carboxylic acids, hydrophobic associations occur intra- and intermolecularly, resulting in the folding of the polymer chain and the formation of hydrophobic microdomains incorporating a number of carboxylic acid groups. In these polymer aggregates, the mobility of the polymer main chain and aromatic rings is extremely restricted. It is likely that these polymer aggregates formed at pH ≈ 5 are mesoglobules (or globules) reported by Timoshenko et al. [15]. In addition, the apparent cmc determined for pMPhe at pH ≈ 5 by steady-state fluorescence may correspond to the boundary between globule and mesoglobule phases [15].

The C_p dependencies of association properties of pMPhe and pMTrp at pH ≈ 5 are distinct. Steady-state fluorescence data using pyrene (Figs. 5(a) and 7) indicated that I_{338}/I_{333} started to increase at lower C_p for pMPhe than for pMTrp. These data indicate that pMPhe is more hydrophobic microscopically than pMTrp, consistent with the solubilities in water for model compounds (i.e., benzene and indole, respectively) of the substituents in Phe and Trp [16]. On the other hand, DLS data (Fig. 10) indicated that pMTrp had a stronger tendency for interpolymer association than pMPhe did. These data corresponds to the observation that pMTrp is less soluble in acidic media than pMPhe, contrast to the solubilities of the substituent model compounds. Since the polymer chains are folded at pH ≈ 5, the difference in the degree of the folding of polymer chains may cause the distinction in the tendency for interpolymer association. It is considered that pMTrp chains are folded less tightly than pMPhe chains, because pMTrp-carrying (3-indolyl)methyl groups are more bulky and less hydrophobic than pMPhe-carrying benzyl groups. This may be why pMTrp exhibits a stronger tendency for interpolymer association. Therefore, it is concluded that the self-association behavior of these polymers is dependent on the bulkiness and the hydrophobicity of the substituent of amino acid residue.

Successful utilization of such subtle differences in side chains may allow us to control precisely and delicately the self-association behavior of synthetic polymers.

Acknowledgements

The authors would like to express their acknowledgment to Professor Takahiro Sato, Department of Macromolecular Science, Graduate School of Science, Osaka University, for fruitful discussion and suggestions. The authors also thank Mr Seiji Adachi, Department of Chemistry, Graduate School of Science, Osaka University, for NOESY measurements.

References

[1] For example (a) Creighton TE. Proteins. Structures and molecular properties. 2nd ed. New York: W.H. Freeman; 1993.
(b) Voet D, Voet JG. Biochemistry. 2nd ed. New York: Wiley; 1995.
(c) Alberts B, Johnson A, Lewis J, Raff M, Roberts K, Walter P. Molecular biology of the cell. 4th ed. New York: Garland Science; 2002.
[2] For example (a) Kulkarni RK, Morawetz H. J Polym Sci 1961;54: 491–503.
(b) Iwakura Y, Toda F, Suzuki H. J Org Chem 1967;32:440–3.
(c) Wang Y, Labsky J, Morawetz H. Macromolecules 1987;20: 2128–33.
(d) Masuda S, Miyahara T, Minagawa K, Tanaka M. J Polym Sci, Part A: Polym Chem 1999;37:1303–9.
(e) Bentolila A, Vlodavsky I, Haloun C, Domb AJ. Polym Adv Tech 2000;11:377–87.
(f) Bentolila A, Vlodavsky I, Ishai-Michaeli R, Kovalchuk O, Haloun C, Domb AJ. J Med Chem 2000;43:2591–600.
(g) Sanda F, Nakamura M, Endo T, Takata T, Handa H. Macromolecules 1994;27:7928–9.
(h) Sanda F, Endo T. Macromol Chem Phys 1999;200:2651–61.
(i) Morcellet-Sauvage J, Morcellet M, Loucheux C. Makromol Chem 1981;182:949–63.
(j) Morcellet M. Thermochim Acta 1992;195:335–41.
(k) Motherwell WB, Atkinson CE, Aliev AE, Wong SYF, Warrington BH. Angew Chem, Int Ed 2004;43:1225–8.
[3] (a) Methenitis C, Morcellet J, Pneumatikakis G, Morcellet M. Macromolecules 1994;27:1455–60.
(b) Methenitis C, Pneumatikakis G, Pitsikalis M, Morcellet J, Morcellet M. J Polym Sci, Part A: Polym Chem 1995;33:2233–9.
[4] (a) Barbucci R, Casolaro M, Magnani A. Makromol Chem 1989;190: 2627–38.
(b) Barbucci R, Casolaro M, Magnani A, Roncolini C. Macromolecules 1991;24:1249–52.
(c) Casolaro M. Macromolecules 1995;28:2351–8.
[5] Morishima Y, Tominaga Y, Nomura S, Kamachi M. J Polym Sci, Part A: Polym Chem 1993;31:789–96.
[6] Hopp TP, Woods KR. Proc Natl Acad Sci USA 1981;78:3824–8.
[7] Frechet JMJ, Mikes F, Vyprachticky D, Lam H, Labsky J. Makromol Chem 1988;189:671–82.
[8] Fieser LF, Fieser M. Reagents for organic synthesis. New York: Wiley; 1967. p. 191–5.
[9] (a) Jakeš J. Czech J Phys 1988;B38:1305–16.
(b) Jakeš J, Štěpánek P. Czech J Phys 1990;40:972–83.
[10] Wilhelm M, Zhao C-L, Wang Y, Xu R, Winnik MA, Mura J-L, Riess G, Croucher MD. Macromolecules 1991;24:1033–40.
[11] Kalyanasundaram K, Thomas JK. J Am Chem Soc 1977;99:2039–44.
[12] Nakajima A. Bull Chem Soc Jpn 1977;50:2473–4.
[13] Petit-Agnely F, Iliopoulos I, Zana R. Langmuir 2000;16:9921–7.
[14] Nishio M, Hirota M, Umezawa Y. The CH/π interaction: evidence nature, and consequences. New York: Wiley; 1998.
[15] (a) Timoshenko EG, Kuznetsov YA, Dawson KA. Physica A 1997; 240:432–42.
(b) Byrne A, Timoshenko EG, Dawson KA. Physica A 1997;243: 14–24.
[16] Dean JA, editor. Lange's handbook of chemistry. 15th ed. New York: McGraw-Hill; 1999. p. 1.76–1.343.